Supplementary Information

Label-free single-cell antimicrobial susceptibility testing in droplets with concentration gradient generation

Jae Seong Kim[a], Jingyeong Kim[a], Jae-Seok Kim[b], Wooseong Kim[c], and Chang-Soo Lee[a]*

[a] Department of Chemical Engineering and Applied Chemistry, Chungnam National University, Daejeon 3414, South Korea

[b] Department of Laboratory Medicine, Kangdong Sacred Heart Hospital, Hallym University College of Medicine, Seoul 05355, South Korea

[c] College of Pharmacy and Graduate School of Pharmaceutical Sciences, Ewha Womans University, Seoul 03760, South Korea

*Corresponding author: rhadum@cnu.ac.kr

Numerical simulation

We built a model of a microfluidic design without the channel structure for the oil phase to validate the performance of the concentration gradient generation. Two fluids from the inlets are set as 0 and 1 in concentration, 10^3 kg/m^3 in density, 10^{-3} Pa·s in viscosity. The distribution of the liquid is obtained by solving the continuity equation, modified Navier-Stokes equation and associated boundary conditions. The mixing of two solutions is set to be completed in a short distance as indicated by the merged interface as shown in Figure S1.

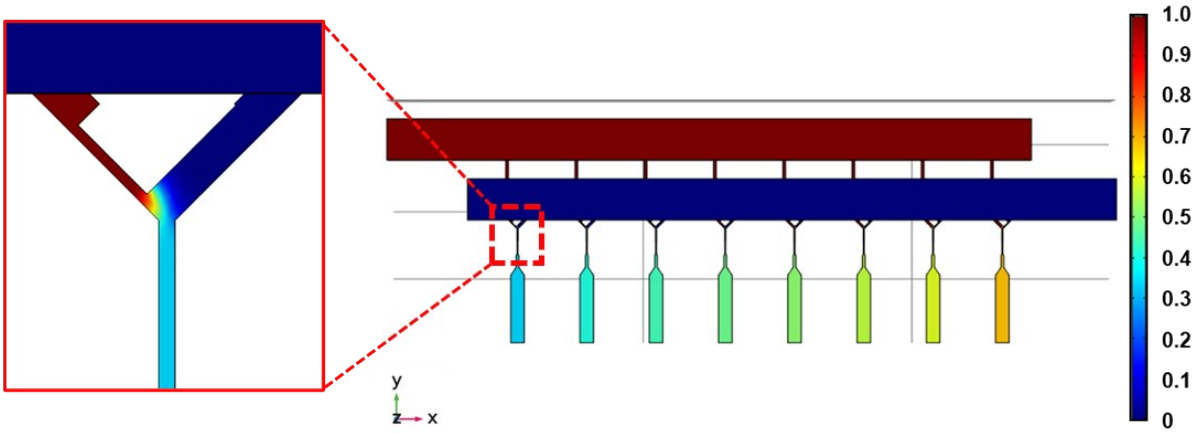

Figure S1 Numerical simulation of the microfluidic device with different widths of channels

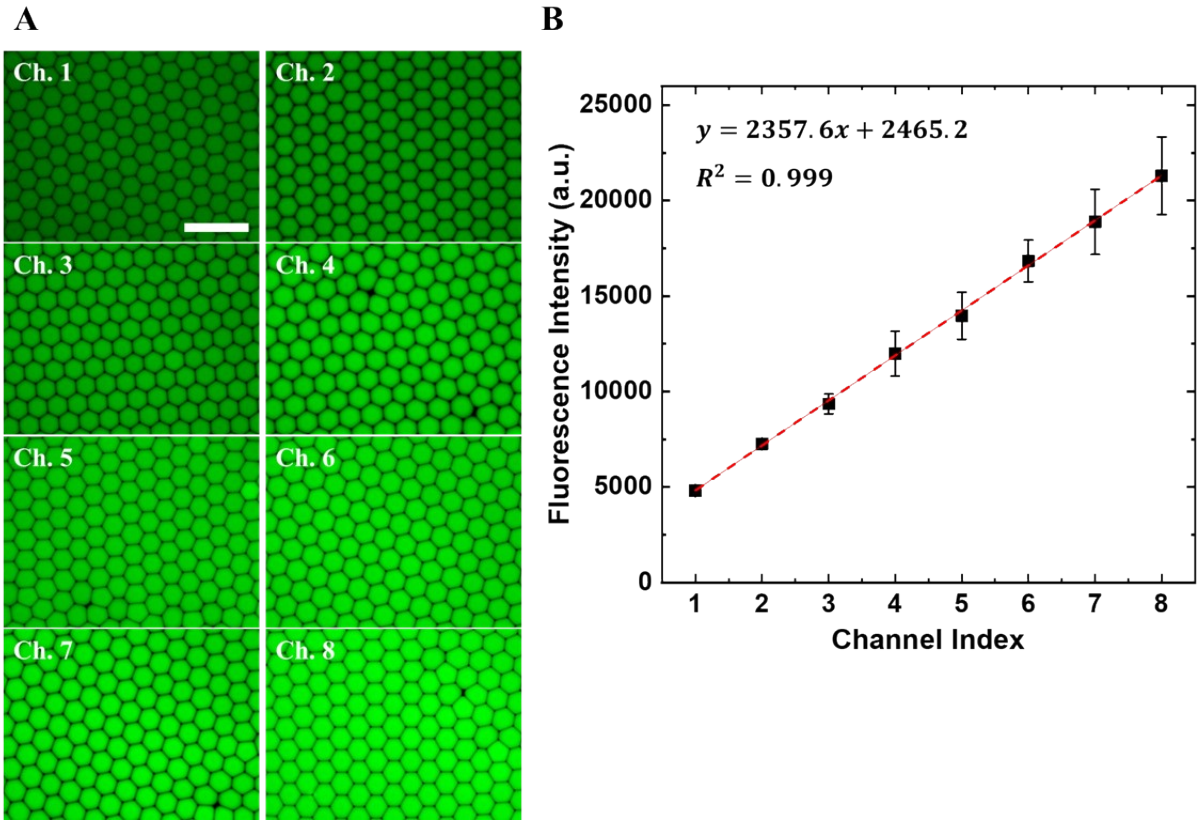

Figure S2 Quantitative analysis of fluorescence intensity of droplets across microfluidic channels. (A) The fluorescence images of droplets in eight channels (from channel 1 to 8). The scale bar indicates 200 μm. (B). A plot for the fluorescence intensity of droplets as a function of the channel index.

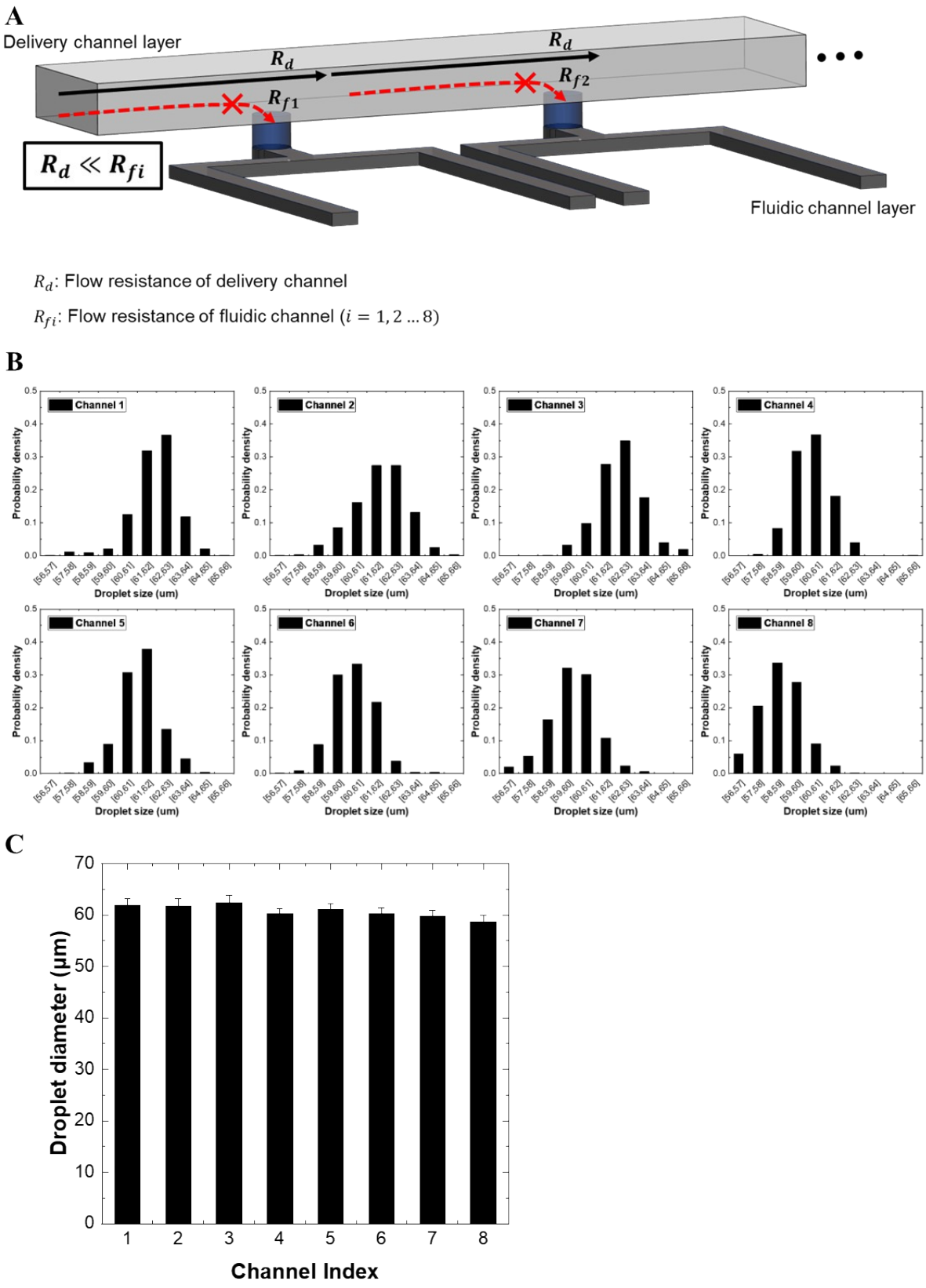

Figure S3 (A) Diagram illustrating the layout of the delivery and fluidic channels within the

microfluidic device, showing the flow resistance, R_d, of the delivery channel is significantly less than the fluidic channel resistance, R_{fi}. This design ensures consistent fluid flow and pressure distribution across all channels (Movie S2). (B) The quantitative analysis shows the size distribution of droplets produced in each of the eight channels, indicating the precision of droplet formation within the device. (C) The average droplet diameter from each channel with error bars representing the standard deviation demonstrates the device's ability to generate monodisperse droplets with high uniformity, which is critical for ensuring reproducibility in microfluidic analyses.

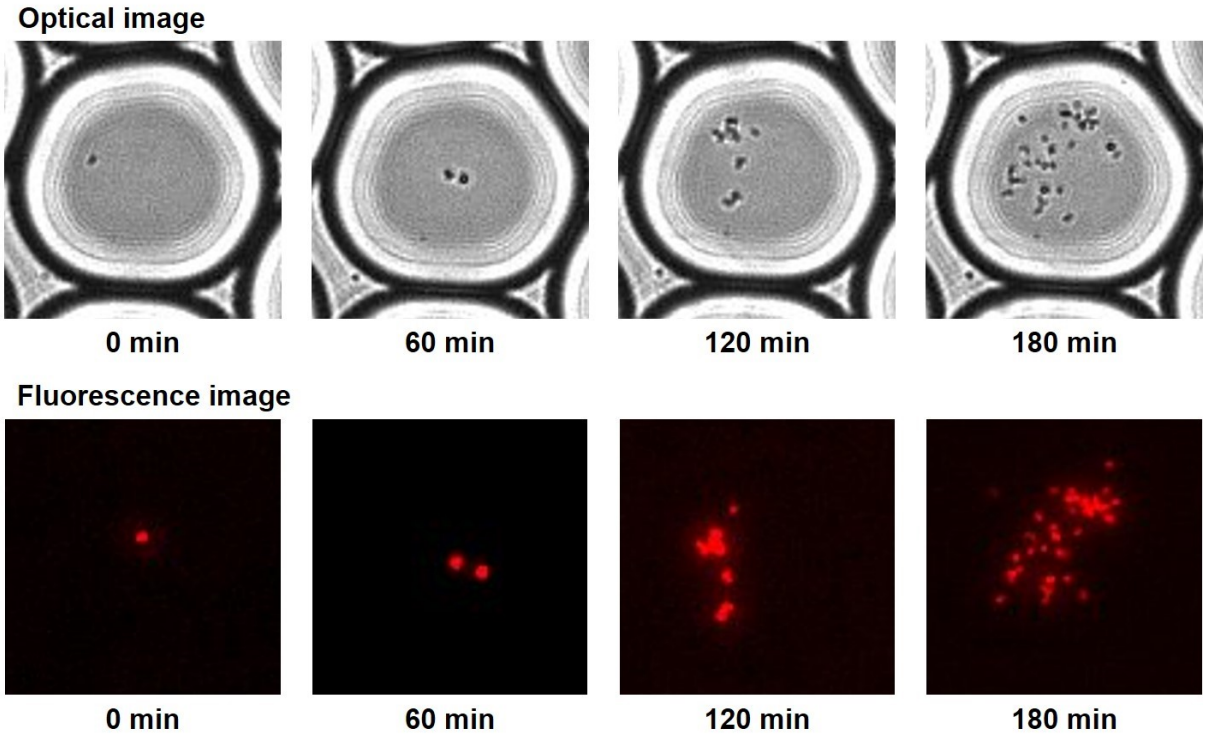

Figure S4 Temporal monitoring of *S. aureus* growth within droplets in the absence of antibiotics. Optical (top row) and fluorescence (bottom row) images captured at 0, 60, 120, and 180 minutes show the progression of bacterial proliferation.

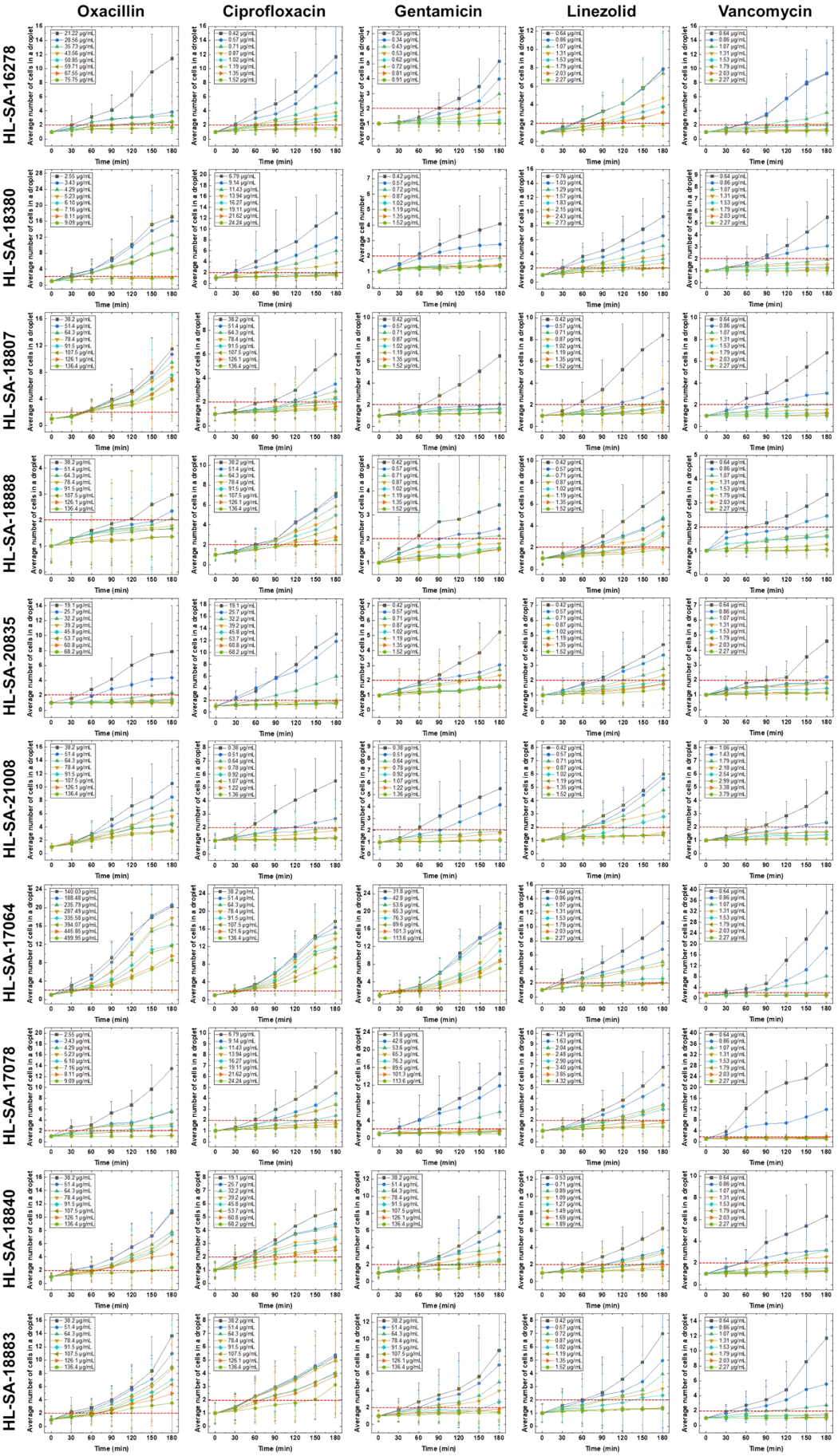
Oxacillin
Ciprofloxacin
Gentamicin
Linezolid
Vancomycin
HL-SA-16278
HL-SA-18380
HL-SA-18807
HL-SA-18888
HL-SA-20835
HL-SA-21008
HL-SA-17064
HL-SA-17078
HL-SA-18840
HL-SA-18883
Average number of cells in a droplet
Average cell number
Time (min)

Figure S5 The determination of MIC of clinical isolates against five CLSI-recommended antibiotics (oxacillin, gentamicin, ciprofloxacin, linezolid, and vancomycin).

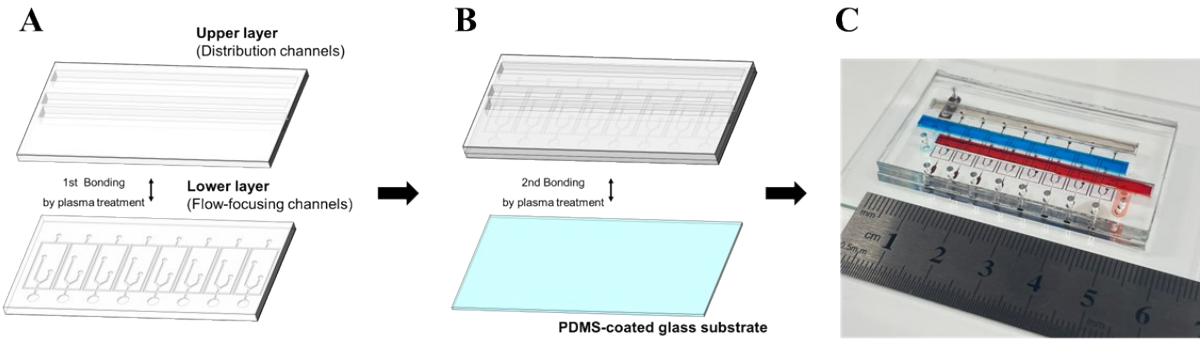

Figure S6 Assembly of the microfluidic device. (A) Microfluidic upper layer and lower layer are bonded each other through the plasma treatment. (B) After punching the inlet and outlet through-holes, the microfluidic device is bonded to a PDMS-coated glass slide. (C) A photograph of the assembled microfluidic device.

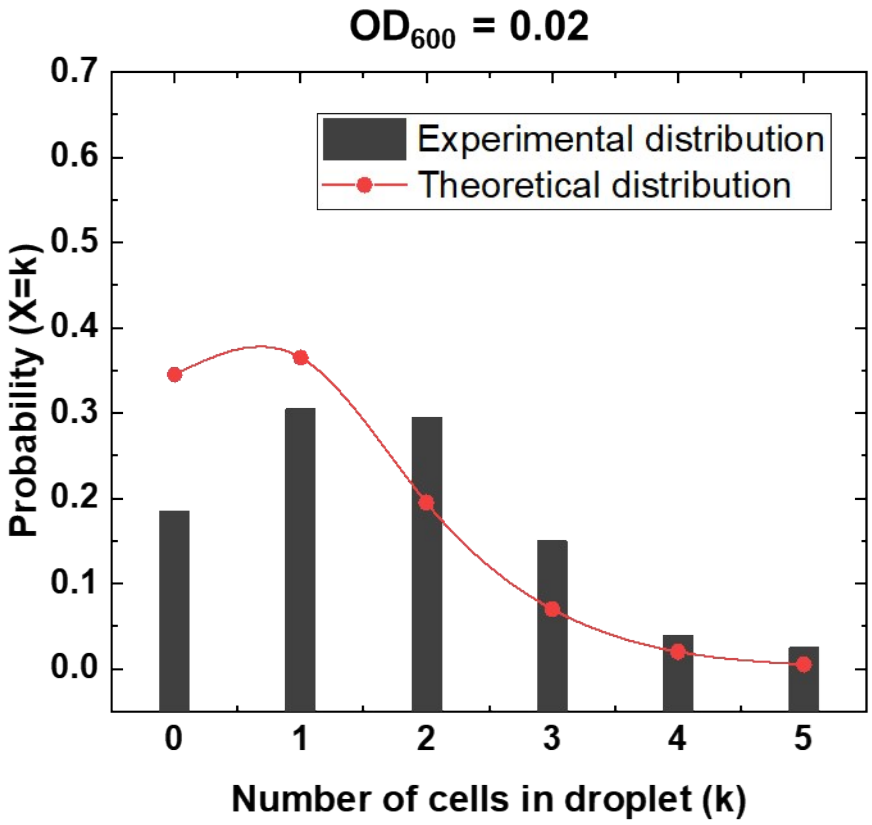

Figure S7. Distribution of the number of bacterial cells encapsulated in droplets.

The figure shows the probability distribution of the number of bacterial cells per droplet after encapsulation from a sample with an optical density (OD) of 0.02. The black bars represent the experimental distribution of cell counts in droplets, obtained from our experiment. The red line with dots represents the theoretical Poisson distribution, which models the expected probability of encapsulating a specific number of cells per droplet. The close agreement between the experimental and theoretical distributions suggests that the encapsulation of bacteria into droplets follows a Poisson process.

Table S1 The BMD assay of clinical isolates.

Type	Bacterial strain	MIC (μg/mL)				
		Oxacillin	Ciprofloxacin	Gentamicin	Linezolid	Vancomycin
Methicillin-resistant *S. aureus*	HL-SA-16278	Resistant*	1	0.5	2	1
	HL-SA-18380	Resistant	16	0.5	2	1
	HL-SA-18807	Resistant	Resistant	0.5	1	1
	HL-SA-18888	Resistant	Resistant	0.5	2	1
	HL-SA-20835	Resistant	32	0.5	2	1
	HL-SA-21008	Resistant	0.125	0.5	2	1
Multidrug-resistant *S. aureus*	HL-SA-17064	Resistant	Resistant	Resistant	1	1
	HL-SA-17078	Resistant	16	Resistant	2	1
	HL-SA-18840	Resistant	32	Resistant	2	1
	HL-SA-18883	Resistant	Resistant	Resistant	2	1

*In this study, “resistant” is defined as clinical isolates exhibiting normal growth at antibiotic concentrations exceeding 64 μg/ml

Supplementary movies

Movie S1. A video showing the stability of concentration gradient generation within the microfluidic channels.

Movie S2. A video showing the generation of monodisperse droplets.